Accepted Manuscript

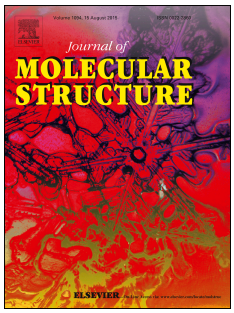

Chemosensing, molecular docking and antioxidant studies of 8-aminoquinoline appended acylthiourea derivatives

A. Kalaiyarasi, J. Haribabu, D. Gayathri, K. Gomathi, N.S.P. Bhuvanesh, R. Karvembu, V.M. Biju

PII: S0022-2860(19)30238-8

DOI: https://doi.org/10.1016/j.molstruc.2019.02.098

Reference: MOLSTR 26255

To appear in: *Journal of Molecular Structure*

Received Date: 24 November 2018

Revised Date: 11 February 2019

Accepted Date: 25 February 2019

Please cite this article as: A. Kalaiyarasi, J. Haribabu, D. Gayathri, K. Gomathi, N.S.P. Bhuvanesh, R. Karvembu, V.M. Biju, Chemosensing, molecular docking and antioxidant studies of 8-aminoquinoline appended acylthiourea derivatives, *Journal of Molecular Structure* (2019), doi: https://doi.org/10.1016/j.molstruc.2019.02.098.

This is a PDF file of an unedited manuscript that has been accepted for publication. As a service to our customers we are providing this early version of the manuscript. The manuscript will undergo copyediting, typesetting, and review of the resulting proof before it is published in its final form. Please note that during the production process errors may be discovered which could affect the content, and all legal disclaimers that apply to the journal pertain.

ACCEPTED MANUSCRIPT

Chemosensing, molecular docking and antioxidant studies of 8-aminoquinoline appended acylthiourea derivatives

A. Kalaiyarasi[a], J. Haribabu[a], D. Gayathri[b], K. Gomathi[c], N. S. P. Bhuvanesh[d], R. Karvembu[a,*], V. M. Biju[a,*]

[a] Department of Chemistry, National Institute of Technology, Tiruchirappalli, 620015, India

[b] Centre of Advanced Study in Crystallography and Biophysics, University of Madras, Guindy Campus, Chennai 600025, India

[c] Department of Biotechnology, Dr. MGR Educational and Research Institute University, Maduravoyal, Chennai 600095, India

[d] Department of Chemistry, Texas A & M University, College Station, TX, 77842, USA

ABSTRACT

Acylthiourea derivatives, 1-benzoyl-3-(quinolin-8-yl)thiourea (**1**), 1-(furan-2-carbonyl)-3-(quinolin-8-yl)thiourea (**2**) and 1-(thiophene-2-carbonyl)-3-(quinolin-8-yl)thiourea (**3**) were synthesized and well characterized by using NMR (^{1}H and ^{13}C), FT-IR, UV-visible and mass spectroscopy tools. The molecular structures of compounds **1** and **3** were confirmed by single crystal X-ray crystallography. The fluorescence emission of the compounds (**1**-**3**) was studied using fluorescence spectrophotometer. The sensing ability of the acylthiourea derivatives was analyzed by colorimetric, UV-visible and fluorescence titrations. *In silico* anti-inflammatory, antimalarial and anti-tuberculosis activities were investigated using molecular docking studies. Acylthiourea derivatives also possessed good antioxidant activity.

Keywords: 8-aminoquinoline, acylthiourea, chemosensor, molecular docking, antioxidant, antimicrobial

*Corresponding authors.

E-mail addresses: vmbiju@nitt.edu (V. M. Biju), kar@nitt.edu (R. Karvembu)

1. Introduction

N-Acylthioureas are promptly synthesized from cheap starting materials in just a single or two stages. Their poisonous quality is very low, and they are stable over fairly long periods**.** Some derivatives of thiourea are biologically active; they show antifungal [1], antitumor [2-4], antiviral, antibacterial [5-7], pharmacological [8], herbicidal and insecticidal properties [5-7]. The aminoquinolines are significant precursors/intermediates in the synthesis of some dyes and drugs. Strikingly, 8-aminoquinoline (8-AQ) derivatives, for example, pamaqune and primaqune have pulled in much enthusiasm as chemotherapeutic and prophylactic operators against the liver phases of Plasmodium vivax and Plasmodium falciparum malarials [8-10]. Antimalarial action of 7-chloroquinolinyl thiourea was reported by Mahajan *et al*. [11].

Numerous transition metal ions are pervasive in nature and they play out several biological functions while in the meantime, overabundance of these ions in bio systems can prompt sicknesses [12]. Hence, multifunctional sensors that create fluorescence or colour response to various metal ions will have more potential in ecological applications [13]. Quinoline derivatives, especially 8-hydroxyquinoline and 8-aminoquinoline, are notable fluorogenic chelator for transition metal ions. In view of the above, we report herein the synthesis, and chemosensing, antioxidant and molecular docking studies of three acylthiourea derivatives bearing quinoline moiety namely, 1-benzoyl-3-(quinolin-8-yl)thiourea (**1**), 1-(furan-2-carbonyl)-3-(quinolin-8-yl)thiourea (**2**) and 1-(thiophene-2-carbonyl)-3-(quinolin-8-yl)thiourea (**3**).

2. Experimental

2.1 Materials and methods

Required chemicals were purchased from Sigma Aldrich/Merck and utilized as received. Solvents were purified by the standard methods. The melting points were determined on Lab India Instrument and are uncorrected. FT-IR spectra were recorded as KBr pellets on a Nicolet-iS5 spectrophotometer. UV-Vis spectra were recorded using a Shimadzu-2600 spectrophotometer. NMR spectra were recorded in DMSO-d_6 or $CDCl_3$ using TMS as an internal standard on a Bruker 500 MHz spectrometer. Thermo exactive Orbitrap mass spectrometer was used to record mass spectra of the compounds. Fluorescence experiments were carried out at room temperature using Fluromax-P high performance research and analytical spectrofluorometer/phosphorimeter. The fluorescence of the compounds with metal ions was observed in 10 µM solution in DMSO at the excitation

wavelength of 343 nm. Life time of the compounds was measured using Horiba instrument. The antioxidant potential of the acylthiourea derivatives was tested using the DPPH free radical scavenging method [14]. Blood biocompatibility of the compounds was studied using haemolysis method [15].

2.2 Synthesis

Benzoyl chloride, furan-2-carbonyl chloride or thiophene-2-carbonyl chloride (0.01 mol) in 50 mL of acetone was slowly added to the suspension of KSCN (0.971 g, 0.01 mol) in 50 mL of anhydrous acetone. The resultant mixture was refluxed for 1 h and allowed to cool at room temperature. 8-Aminoquinoline dissolved in 40 mL of acetone (1.442 g, 0.01 mol) was added dropwise and the solution was stirred for 2 h at room temperature. HCl (0.1 N, 600 mL) was added and the product separated was filtered off, washed with water and dried *in vacuo*. Single crystals of acylthiourea derivatives for XRD analysis were grown at room temperature from their CH_3CN solutions.

*2.2.1 1-Benzoyl-3-(quinolin-8-yl)thiourea (**1**)*

Yield: 71%. Yellow solid. M.p.: 184 °C. UV-Vis (DMSO): λ_{max}, nm (ε, $dm^3mol^{-1}cm^{-1}$) 281 (94832), 337 (64828). FT-IR (KBr): υ, cm^{-1} 3312 (N–H), 3040 (H–N–C=S), 1677 (C=O), 1244 (C=S). ^{1}H NMR (500 MHz, $CDCl_3$): δ, ppm 14.47 (s, 1H, NH), 9.67 (d, *J* = 7.7 Hz, 1H, Ar-H), 9.17 (s, 1H, NH), 9.04 (d, *J* = 4.1 Hz, 1H, Ar-H), 8.25 (dd, *J* = 27.8, 8.0 Hz, 2H, Ar-H), 8.00 (d, *J* = 8.1 Hz, 1H, Ar-H), 7.79-7.46 (m, 5H, Ar-H). ^{13}C NMR (125 MHz, DMSO-d_6): δ, ppm 177.65 (C=S), 168.19 (C=O), 149.66, 139.83, 137.20, 135.03, 133.57, 132.71, 129.29, 128.91, 128.34, 126.69, 124.95, 122.93 and 119.52 (aromatic carbons). ESI-MS found m/z = 308.0852 $[M+H]^+$, calcd. 307.3696.

*2.2.2 1-(Furan-2-carbonyl)-3-(quinolin-8-yl)thiourea (**2**)*

Yield: 63%. Yellow solid. M.p.: 176 °C. UV-Vis (DMSO): λ_{max}, nm (ε, $dm^3mol^{-1}cm^{-1}$) 297 (41164), 337 (19056). FT-IR (KBr): υ, cm^{-1} 3400 (N-H), 3148 (H-N-C=S), 1684 (C=O), 1270 (C=S). ^{1}H NMR (500 MHz, $CDCl_3$): δ, ppm 14.26 (s, 1H, NH), 9.68 (d, *J* = 7.7 Hz, 1H, Ar-H), 9.27 (s, 1H, NH, Ar-H), 9.01 (d, *J* = 4.1 Hz, 1H, Ar-H), 8.20 (d, *J* = 8.2 Hz, 1H, Ar-H), 7.88-7.13 (m, 5H, Ar-H), 6.70-6.45 (m, 1H, Ar-H). ^{13}C NMR (126 MHz, $CDCl_3$): δ, ppm 175.34 (C=S), 155.88 (C=O), 149.16, 146.20, 145.32, 140.00, 136.36, 134.94, 128.10, 126.48, 124.30, 121.91, 118.85, 118.82 and 113.40 (aromatic carbons). ESI-MS found m/z = 298.0646 $[M+H]^+$, calcd. 297.3317.

*2.2.3 1-(Thiophene-2-carbonyl)-3-(quinolin-8-yl)thiourea (**3**)*

Yield: 59%. Yellow solid. M.p.: 178 °C. UV-Vis (DMSO): λ_{max}, nm (ε, $dm^3mol^{-1}cm^{-1}$) 298 (36516), 337 (18584). FT-IR (KBr): υ, cm^{-1} 3270 (N-H), 3062 (H-N-C=S), 1663 (C=O), 1244 (C=S). ^{1}H NMR (500 MHz, $CDCl_3$): δ, ppm 14.21 (s, 1H, NH), 9.65 (d, *J* = 7.7 Hz, 1H, Ar-H), 9.02 (s, 1H, NH), 8.21 (d, *J* = 8.2 Hz, 1H, Ar-H), 7.79 (d, *J* = 3.7 Hz, 1H, Ar-H), 7.72-7.50 (m, 5H, Ar-H), 7.20 (t, *J* = 4.3 Hz, 1H, Ar-H), ^{13}C NMR (126 MHz, $CDCl_3$): δ, ppm 175.47 (C=S), 159.99 (C=O), 149.25, 140.05, 136.42, 136.36, 134.89, 133.99, 130.67, 128.40, 128.11, 126.45, 124.39, 121.92, 118.99 (aromatic carbons). ESI-MS found m/z = 314.0417 $[M+H]^+$, calcd. 313.3973.

2.3 X-ray crystallography

Crystal structures of the two quinolone based acylthiourea compounds (**1** and **3**) have been confirmed by using X-ray diffraction. The single crystal data collection and structure refinement details of the two quinolone based acylthiourea compounds (**1** and **3**) are provided in Table 1. The data of acylthiourea compounds **1** and **3** were collected at 100 K by Bruker Venture diffractometer (kappa geometry) utilizing a Cu-Iμs X-ray tube (K_α= 1.5418 Å). Integrated intensity information for each reflection was obtained by reduction of the data frames with the program APEX3 [16]. The integration method employed a three dimensional profiling algorithm and all data were corrected for Lorentz and polarization factors as well as for crystal decay effects. Finally, the data were merged and scaled to produce a suitable data set. SADABS [17] was employed to correct the data for absorption effects. A solution was obtained readily using XT/XS in APEX3 [18]. The H atoms were added at the calculated positions in the final refinement cycles. All non-H atoms were refined with the anisotropic thermal parameters. The structure was refined (weighted least squares refinement) on F^2 to convergence [18,19].

2.4 Sensing studies

The UV-Vis absorption spectra were acquired from the DMSO solutions of the samples in a 1 cm quartz cell in the range of 200-700 nm at room temperature. Each sample solution was prepared from 1 mM stock solution of the compounds in DMSO and diluted to the desired concentration with DMSO. The 1 mM stock solution of the cations tested was prepared by dissolving the salts such as sulphates of Mg(II), Zn(II), Cu(I), Cu(II) and Al(III), acetates of Cd(II) and Hg(II), nitrates of Pb(II) and Co(II), and chlorides of Ni(II), Mn(II), Fe(II), Fe(III), and Cr(III) in Milli-Q water.

The fluorescence spectrum was obtained from the solution in 3.5 mL fluorescence quartz cell with 1 cm optical path length at ambient temperature and an excitation wavelength of 338 nm.

2.5 Molecular docking studies

In silico induced fit molecular docking studies were performed using Schrodinger-Maestro [20] (Schrodinger LLC 2009, USA) to evaluate the binding mode of the compounds with phospholipase A2, lactate dehydrogenase and decaprenylphosphoryl-D-ribose oxidase enzymes. Energy minimized three dimensional structures of the compounds were generated by Ligprep. Three dimensional coordinates of the enzymes were downloaded from RCSB Protein Data Bank [21] followed by energy minimization in order to account for adding hydrogen atoms, assigning proper bond orders, ionization states along with charge fixing. Energy minimized compounds were subjected to induced fit molecular docking at the active site of the enzymes and the best docked conformation was analysed in terms of docking score, energy, hydrogen bonding and hydrophobic interactions. Protein-ligand interactions are represented by Ligplot using PDBSUM [22]. Cartoon/surface view representations of enzyme with ligand bound at the active site were generated with PyMol [23].

3. Results and discussion

3.1 Synthesis and characterization

Quinolin-8-yl thiourea derivatives (**1-3**) were prepared from acid chloride (furan-2-carbonyl chloride / thiophene-2-carbonyl chloride / benzoyl chloride), potassium thiocyanate and 8-aminoquinoline in dry acetone (Scheme 1) [24]. The acylthiourea compounds (**1-3**) showed two bands at 281-298 and 337-338 nm in their UV-Visible spectra, which were characteristic of π-π^* and n-π^* transitions respectively. In their FT-IR spectra, strong bands appeared around 3400-3270 and 3148-3010 cm^{-1}, which were attributed to amide N–H and H–N–C=S respectively. The carbonyl and thiocarbonyl stretching bands appeared at 1684-1663 and 1251-1244 cm^{-1} respectively. In the ^{1}H NMR spectra of **1-3**, the carbonyl attached and thiocarbonyl attached NH protons were observed in the regions 14.47-14.21 and 9.68-9.65 ppm respectively. Signals due to aromatic protons appeared at 9.04-6.64 ppm. ^{13}C NMR spectra showed signals at 175.6-175.3 and 168.1-155.5 ppm which were due to C=S and C=O carbons respectively. The signals around 149.7-149.2 ppm were assigned to the aromatic carbons (Fig S1-S6) [25].

Crystal structures of the acylthiourea derivatives (**1** and **3**) were determined by XRD technique. The crystals of two acylthiourea compounds **1** and **3** grown at room temperature from their CH_3CN solutions were found to be suitable for single crystal X-ray diffraction analysis. Three dimensional molecular structures of two acylthiourea compounds (**1** and **3**) are displayed in Figs. 1 and 2. Crystallographic data and refinement parameters are given in Table 1. CIF files have been deposited in Cambridge structure database (CCDC 1875313 and 1875314). The selected bond lengths and angles of compounds **1** and **3** are provided in Table 2 and were comparable with the similar thiourea compounds reported [25]. Table 3 shows torsion angles for compounds **1** and **3**. An intra molecular hydrogen bonding was found between carbonyl oxygen and thiocarbonyl attached NH (O…HN) with bond distance of 2.6304(15) (**1**) and 2.650(2) (**3**) Å (Table 4).

3.2 Visual detection, UV-Vis absorbance and fluorescence studies

The visual detecting ability of the compounds (**1-3**, 1 mM) towards cations (1 mM) such as Mg(II), Zn(II), Cd(II), Hg(II), Pb(II), Co(II), Ni(II), Mn(II), Fe(II), Cu(I), Cu(II), Fe(III), Al(III), and Cr(III) was analyzed by colorimetric method. Colour of compounds **1-3** was changed to pale yellow upon addition of Ni(II), Co(II), Zn(II), Cu(I), Fe(II) and Fe(III), yellow on addition of Cu(II), and soiled yellow with Hg(II) ion. Figs. S7-S9 reveal colour changes of compounds **1-3** in the absence and presence of various metal ions. The negligible colour changes induced by the other metal ions tested indicated that compounds **1-3** could selectively recognize a range of metal ions such as Ni(II), Co(II), Zn(II), Cu(I), Fe(II), Fe(III), Cu(II) and Hg(II).

The sensing behaviour of compounds **1-3** towards cations was additionally examined by UV-Vis spectroscopy. UV-Vis spectra were recorded while adding the metal ions (up to 100 µL from 1 mM solution) into compounds **1-3** (1 mM). Figs. S10-S12 illustrate the spectral changes upon addition of different metal ions to the compounds (**1-3**). With Hg(II), all the compounds showed an increase in absorbance along with red shift in n-π* transition. Compounds **1-3** showed a new band around 400 nm when Cu(I), Ni(II), Zn(II) or Cu(II) ion was added. This indicated that these ions formed complexes with the acylthiourea derivatives. With the other metal ions tested, only negligible shifts in the absorbance values were observed.

The steady-state fluorescence emission spectra of compounds **1-3** were recorded and found to be similar. The maximum emission wavelength of the compounds was in the range 450-500 nm. A phenomenal red shift of emission wavelength was noticed for all the compounds Fig S13. The fluorimetric behaviour of compounds **1-3** in DMSO was

investigated upon addition of aqueous solution of metal ions such as Mg(II), Zn(II), Cd(II), Hg(II), Pb(II), Co(II), Ni(II), Mn(II), Fe(II), Cu(I), Cu(II), Fe(III), Al(III) and Cr(III). Interestingly, ten-fold increase in fluorescence intensity with red shift was seen with Zn(II) ion. Marginal fluorescent enhancement accompanied by blue shift was observed with Hg(II), Cd(II) and Mg(II) ions. Fluorescence quenching was observed while adding the other metal ions. Hence, it was confirmed that the acylthiourea derivatives can act as fluorescent chemosensors for Zn(II) ion. Moreover, Hg(II), Cd(II) and Mg(II) ions may also be detected (Figs. 3-5).

Figs. S14-S16 demonstrate the fluorescence spectra of **1-3** in water/DMSO (3:97% v/v), with different concentrations of Zn(II) ion. They were recorded with an excitation at 343 nm. Without Zn(II) ion, compounds **1-3** produced weak fluorescence around 450-500 nm. On the introduction of Zn(II), another emission band at 520 nm was shown. Moreover, the emission intensity gradually increased with the increasing Zn(II) ion concentration. Further, the emission band was red-shifted with the increasing concentration of Zn(II) ions; red-shift of 70 nm was observed with 2.5×10^{-6} M Zn(II). The detection limit for compounds **1-3** with Zn(II) was found to be 6, 5.3 and 5.6 µM respectively [26]. These values are about 13 fold lower than that prescribed in WHO guidelines (~76 µM) for drinking water, indicating that compounds **1-3** can act as efficient fluorogenic chemosensor for Zn(II) recognition [27]. The UV-Vis spectral changes ascribed to the coordination of Zn(II) with the acylthiourea derivatives. After the compound binds with Zn(II), the intramolecular hydrogen bond in the compound breaks, and the intramolecular electron transfer is forbidden which enhances the fluorescence emission [28].

To determine the stoichiometry, solutions were prepared at different ratios of **1-3** and Zn^{2+} (0:10, 1:9, 2:8, 3:7, 4:6, 5:5, 6:4, 7:3, 8:2, 9:1), and their absorbance was measured at 343 nm. When Zn^{2+} was close to 40%, higher absorbance was noted with compounds **1**, **2**, and **3** separately (Fig S17- S19). This demonstrated approximately 2:1 stoichiometry between the compounds and Zn^{2+} (Scheme 2).

3.3 Molecular docking analysis

Thiourea derivatives possess wide range of biological properties like antioxidant, anti-inflammatory, antibacterial, antiviral, antimalarial, etc. *In silico* screening of the compounds has been carried out using molecular docking studies to reveal their biological properties and binding mode at the active site of the enzymes. Three enzymes were chosen for the present *in silico* studies; non pancreatic phospholipase A2, lactate dehydrogenase and

decaprenylphosphoryl-D-ribose oxidase to screen the antiinflammatory, antimalarial and antituberculosis potential, respectively, of the synthesized compounds.

3.3.1 Phospholipase A2

Phospholipase A2 (PLA2), an essential enzyme in lipid signalling, inflammation and immune response, hydrolyzes the phospholipids to form fatty acid and lysophospholipids. The released fatty acid being mostly arachidonic acid is the precursor of the eicosanoid family and the increase in the concentration of eicosanoids leads to various inflammatory responses. Compounds that inhibit PLA2 may act as potent anti-inflammatory compounds as the inhibition of an enzyme leads to decrease in the concentration of eicosanoids. Structural coordinates of human non-pancreatic secretoary PLA2 were downloaded from protein data bank (PDB ID: 1DCY) [29]. Based on the induced fit docking results, it was clearly evident that the compounds bound efficiently; comparable with the co-crystal ligand, indicating that the compounds might possess good anti-inflammatory property. For comparing the docked results of the compounds, 1-benzyl-5-methoxy-2-methyl-1H-indol-3-yl-acetic acid (co-crystal ligand) was re-docked at the active site of PLA2. Docking energy, glide score and active site interactions are listed in Table 5, which are comparable with those reported in the literature [29, 30]. Hydrogen bonding and hydrophobic interactions at the active site of PLA2 are shown by Ligplot representation in Fig. 6. Cartoon representation of PLA2 with compound **1** bound at the active site pocket is shown in Fig. 7.

3.3.2 Lactate dehydrogenase

Plasmodium falciparum lactate dehydrogenase, one of the potential molecular targets for antimalarial drug designing, catalyzes the interconversion of pyruvate and lactate in the glycolysis pathway with concomitant interconversion of NADH and NAD^+. Three dimensional structural coordinates of *P. falciparum* lactate dehydrogenase were downloaded from protein data bank (PDB: 1LDG, [31]) and compounds **1**, **2** and **3** were subjected to molecular docking. Mefloquine [32] was used as a control. Docking energy and glide score of mefloquine, compounds **1**, **2** and **3**, are listed in Table 5. Compound **3** showed better binding energy, score and active site interactions when compared with mefloquine. Mefloquine showed hydrogen bonds with residues Thr97 and Thr101, and hydrophobic interactions with Gly29, Met30, Ile31, Gly99, Phe100, Val138, Thr139, Ser245, Pro246 and Tyr247. Compound **3** was found to possess hydrogen bonds with Thr97, Thr101 and Asn140, and hydrophobic interactions with Met30, Ile31, Gly99, Phe100, Val138, Leu163, Leu167, His195, Ser245, Pro246 and Pro250 residues. Fig. 8 shows the Ligplot representation of

hydrogen bonds and hydrophobic interactions with lactate dehydrogenase enzyme. Fig. 9 shows the surface view of the enzyme bound with compound **3**.

3.3.3 Decaprenylphosphoryl-D-ribose oxidase

Flavo enzyme DprE1, decaprenylphosphoryl-D-ribose oxidase enzyme, catalyzes an important epimerization step in the decaprenylphosphoryl-D-arabinose (DPA) pathway which is essential for mycobacterial cell wall biogenesis, cell wall metabolism, cell growth and cell survival. DprE1 is considered as one of the most vulnerable targets of mycobacterium tuberculosis as it is essential for mycobacterial cell wall biogenesis. Based on the importance of enzyme DprE1, the binding affinity of the three acylthiourea derivatives at the active site of DprE1 was identified through *in silico* induced fit molecular docking studies. Three-dimensional structural coordinates of DprE1 were downloaded from protein data bank (PDB ID: 4FDO) [33] and energy minimized using protein preparation wizard in Schrodinger-Maestro. Co-crystal ligand, 3-nitro-N[(1R)-1-phenylethyl]-5-(trifluoromethyl)benzamide, has been re-docked at the active site of DprE1 to compare the binding energy, glide score and active site interactions with those of the three compounds. Based on the docking energy, glide score, hydrogen bonds and hydrophobic interactions (Table 5), it was observed that all the compounds showed good docking energy and score as compared to the co-crystal ligand. Interactions of the three compounds with the active site residues were found to be better than those of co-crystal ligand. The active site interactions and binding modes of the compounds were comparable with those of the reported compounds [33-35]. Fig. 10 shows the Ligplot representation of active site interactions. Fig. 11 shows the cartoon representation of compound **1** at the active site of DprE1.

3.4 DPPH assay

Wide range of metabolic reactions happening inside the system indirectly accumulates reactive oxygen species (ROS) [36]. The mount up of ROS inside the body plays pathogenic role by initiating various metabolic disorders. Even though anti-oxidative protective system inside our body encounters these ROS, sometimes the defence network fails [37]. In this scenario external supply of anti-oxidative compounds is needed to overcome the oxidative stress.

The 8-aminiquinoline based acylthiourea compounds were evaluated for their antioxidant potential using DPPH scavenging assay. The IC_{50} value of compounds **1**, **2** and **3** was found to be 10 µg/mL. At the concentration of 500 µg/mL, more than 95 % of the radicals were scavenged by the compounds. Further increase in concentration did not change

the activity of the compounds significantly (Fig. 12). In our earlier work [34], the parent acylthiourea compounds exhibited an IC_{50} value of 250 µg/mL while in the present study, the 8-aminoquinoline derivatives showed an IC_{50} of around 10 µg/mL. From the comparison, it was inferred that 8-aminiquinoline derivatives had 25 times more antioxidant potential than their parent compounds. The increase in antioxidant potency of 8-aminoquinoline compounds may be related to their aromatic or heterocyclic structure. It was also reported in other works that quinoline compounds possessed high antioxidant potential [38, 39].

3.5 Haemolysis assay

The acylthiourea compounds with six different concentrations were examined for their toxicity against red blood cells (RBCs). Results were compared to the control cells treated with triton X, which produced 100 % lysis. The results clearly suggested that the acylthiourea derivatives did not induce any haemolysis. The study also proposes that these compounds can be used for further biological studies as they do not produce any toxicity against RBC (Fig. 13).

4. Conclusion

In the present study, three acylthiourea derivatives were synthesized and characterized by spectroscopic techniques. Three dimensional crystal structures of the two compounds were elucidated. The compounds showed multi-fold turn on fluorescent sensing towards Zn^{2+}. *In silico* molecular docking of the acylthiourea derivatives with PLA2, lactate dehydrogenase and DprE1 showed interactions at the active site similar to the co-crystal ligands indicating that the acylthiourea derivatives may possess antiinflammatory, antimalarial and antituberculosis activities. The acylthiourea derivatives were subjected to *in vitro* DPPH antioxidant and antihaemolytic assays and the results showed that the compounds possess good antioxidant and antihaemolytic activities.

Acknowledgement

J. H. thanks the University Grants Commission for the fellowship (F1-17.1/2012-13/RGNF-2012-13-ST-AND-18716).

References

[1] R. d. Campo, J. J. Criado, R. Gheorghe, F. J. González, M. R. Hermosa, F. Sanz, J. L. Manzano, E. Monte, E. Rodrıguez-Fernández, J. Inorg. Biochem. 98 (2004) 1307-1314.

[2] C. Sacht, M. S. Datt, Polyhedron 19 (2000) 1347-1354.

[3] R. Rulkens, M. P. Coles, T. D. Tilley, Dalton Trans. 5 (2000) 627-628.

[4] W. Hernández, E. Spodine, L. Beyer, U. Schröder, R. Richter, J. Ferreira, M. Pavani, Bioinorg. Chem. Appl. 3 (2005) 299-316.

[5] G. Binzet, H. Arslan, U. Florke, N. Kulcu, N. Duran, J. Coord. Chem. 59 (2006) 1395-1406.

[6] A. Kudelski, Pol. J. Chem. 79 (2005) 1551-1563.

[7] S. Saeed, N. Rashid, M. Ali, R. Hussain, Eur. J. Chem. 1 (2010) 200-205.

[8] A. Shi, T. A. Nguyen, S. K. Battina, S. Rana, D. J. Takemoto, P. K. Chiang, D. H. Hua, Bioorg. Med. Chem. Lett. 18 (2008) 3364-3368.

[9] G. D zimbeg, B. Zorc, M. Kralj, K. Ester, K. Paveli, G. Andrei, R. Snoeck, J. Balzarini, E. D. Clercq, M. Mintas, Eur. J. Med. Chem. 43 (2008) 1180-1187.

[10] N. Vale, R. Moreira, P. Gomes, Eur. J. Med. Chem. 44 (2009) 937-953.

[11] A. Mahajan, S. Yeh, M. Nell, C. E. V. Rensburg, K. Chibale, Bioorg. Med. Chem. Lett. 17 (2007) 5683-5685.

[12] B. K. Paul, S. Kar, N. Guchhait, J. Photochem. Photobiol. A 220 (2011) 153-163.

[13] R. Azadbakhta, H. Keypour, Spectrochim. Acta Part A 85 (2012) 293-297.

[14] J. Haribabu, K. Jeyalakshmi, Y. Arun, N. S. P. Bhuvanesh, P. T. Perumal, R. Karvembu, J. Biol. Inorg. Chem. 22 (2017) 461-480.

[15] J. Haribabu, G. Sabapathi, M. Muthu Tamizh, C. Balachandran, N. S. P. Bhuvanesh, P. Venuvanalingam, R. Karvembu, Organometallics 37 (2018) 1242-1257.

[16] APEX3 "*Program for data collection and integration on area detectors*", Bruker AXS Inc., 5465 East Cheryl Parkway, Madison, WI 53711-5373 USA.

[17] G. M. Sheldrick, "*SADABS (version 2016/2): Program for absorption correction for data from area detector frames*", University of Göttingen, 2008.

[18] G. M. Sheldrick, Acta Cryst. A64 (2008) 112-122.

[19] O. V. Dolomanov, L. J. Bourhis, R. J. Gildea, J. A. K. Howard, H. Puschmann, J. Appl. Cryst. 42 (2009) 339-341.

[20] Maestro (Schrodinger LLC 2009, USA).

[21] H. M. Berman, J. Westbrook, Z. Feng, G. Gilliland, T. N. Bhat, H. Weissig, I. N. Shindyalov, P. E. Bourne, Nucl. Acids Res. 28 (2000) 235-242.

[22] R. A. Laskowski, Bioinformatics 23 (2007) 1824–1827.

[23] The PyMOL Molecular Graphics System, Version 1.5.0.4 Schrödinger LLC.

[24] M. Mary Sheeba, M. Muthu Tamizh, S. Ganesh Babu, N. S. P. Bhuvanesh, R. Karvembu, RSC Adv. 6 (2016) 68494-68503.

[25] A. Saeed, U. Flörke, M. F. Erben, J. Sulfur Chem. 35 (2014) 318-355.

[26] F. Sun, G. Zhang, D. Zhang, L. Xue, H. Jiang, Org. Lett. 13 (2011) 6378-6381.

[27] Z. M. Dong, W. Wang, L. Y. Qin, J. Feng, J. N. Wang & Y. Wang, J. Photochem. Photobiol. A 335 (2017) 1-9

[28] K. Boonkitpatarakul, A. Smata, K. Kongukool, S. Srisurichan, K. Chainok, M. Sukwattanasinitt, J. Lumin. 198 (2018) 59-67.

[29] R. W. Schevitz, N. J. Bach, D. G. Carlson, N. Y. Chirgadze, D. K Clawson, R. D. Dillard, S. E. Draheim, L. W. Hartley, N. D. Jones, E. D. Michelich, J. L. Olkowski, D. W. Snyder, C. Sommers, J. P. Wery, Nat. Struct. Biol. 2 (1995) 458-465.

[30] G. R. Subhashree, J. Haribabu, S. Saranya, P. Yuvaraj, D. Anantha Krishnan, R. Karvembu, D. Gayathri, J. Mol. Struct. 1145 (2017) 160-169.

[31] C. R. Dunn, M. J. Banfield, J. J. Barker, C. W. Higham, K. M. Moreton, D. Turgut-Balik, R. L. Brady, J. J. Holbrook, Nat. Struct. Mol. Biol. 3 (1996) 912-915.

[32] V. F. Waingeh, A. T. Groves, J. A. Eberle, Biophys. J. 3 (2013) 285-290.

[33] S. M. Batt, T. Jabeen, V. Bhowruth, L. Quill, P. A. Lund, L. Eggeling, L. J. Alderwick, K. Futterer, G. S. Besra, Proc. Natl. Acad. Sci. USA. 109 (2012) 11354-11359.

[34] J. Haribabu, G. R. Subhashree, S. Saranya, K. Gomathi, R. Karvembu, D. Gayathri, J. Mol. Struct. 1094 (2015) 281–291.

[35] M. H. Shaikh, D. D. Subhedar, B. B. Shingate, F. A. Kalam Khan, J. N. Sangshetti, V. M. Khedkar, L. Nawale, D. Sarkar, G. R. Navale, S. S. Shinde, Med. Chem. Res. 25 (2016) 790-804.

[36] V. López , S. MartÃn, M. P. Gómez-Serranillos, M. E. Carretero, A. K. Jäger, M. I. Calvo, Neurochem. Res. 34 (2009) 1955-1961.

[37] B. Halliwell, J. M. Gutteridge, *Free radicals in biology and medicine*, Oxford University Press, 2015.

[38] M. O. Puskullu, H. Shirinzadeh, M. Nenni, H. Gurer-Orhan, S. Suzen, J. Enzyme Inhib. Med. Chem. 31 (2016) 121–125.

[39] P. Mahajan, M. Nikam, A. Asrondkar, A. Bobade, C. Gill, J. Heterocycl. Chem. 54 (2017) 1415-1422

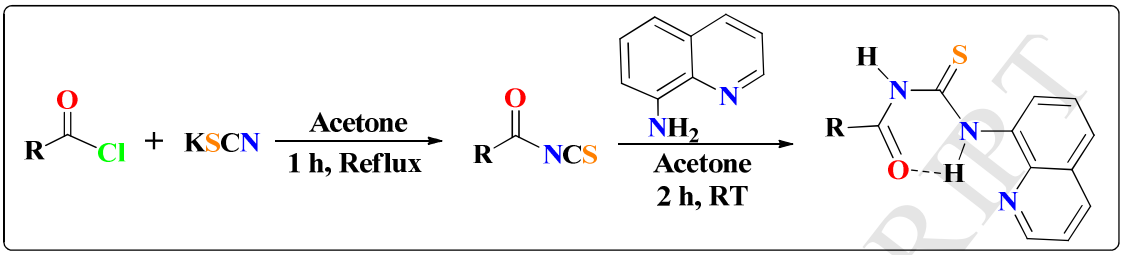

R	Compound
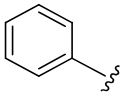	**1**
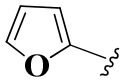	**2**
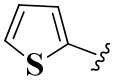	**3**

Scheme 1. Synthesis of compounds **1**-**3**.

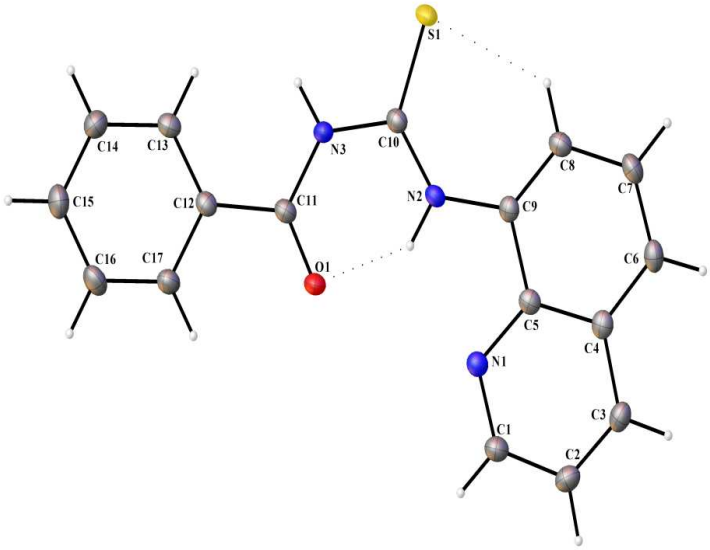

Fig. 1. Molecular struture of **1**.

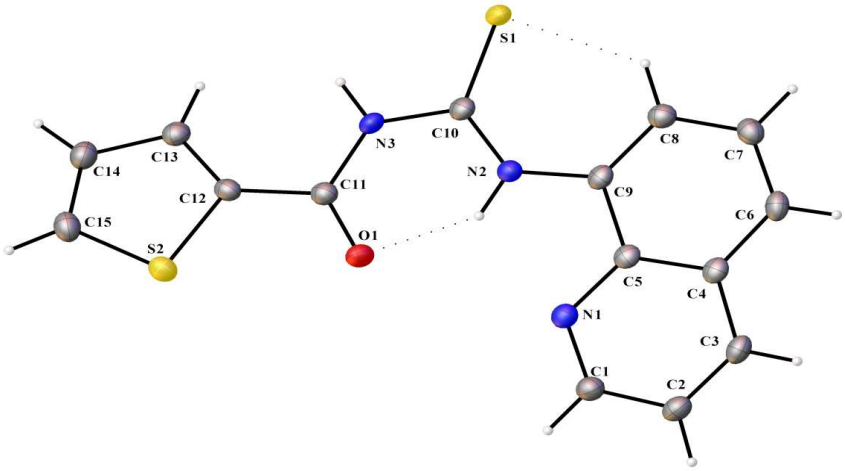

Fig. 2. Molecular structure of **3**.

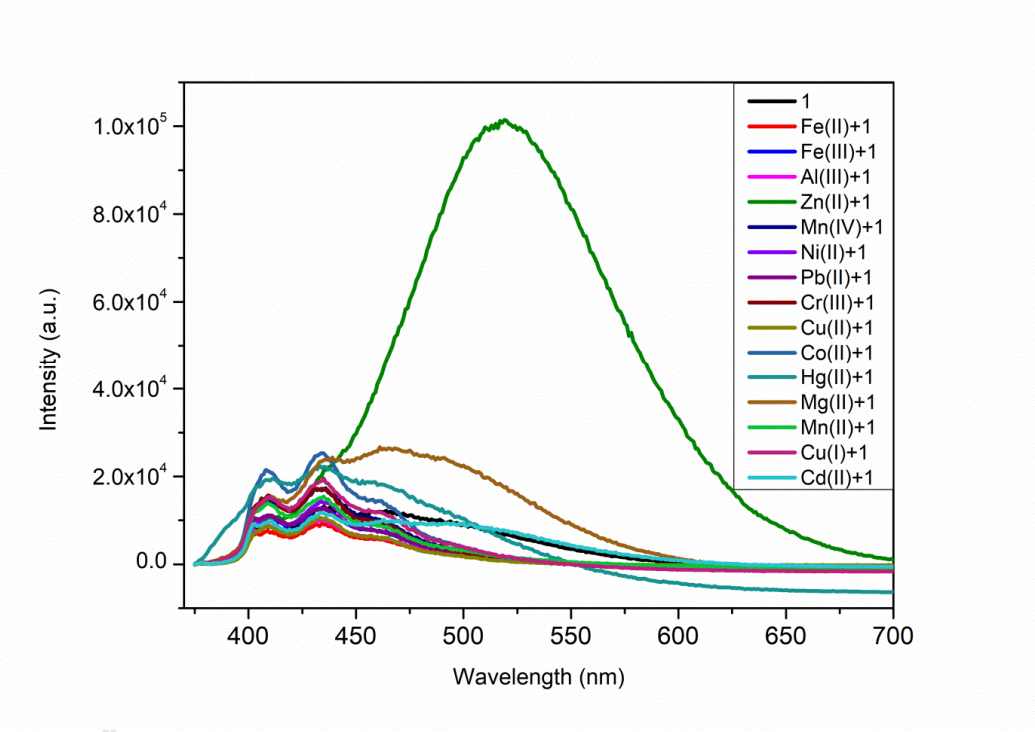

Fig. 3. Fluorescence spectra of **1** with metal ions Mg(II), Zn(II), Cd(II), Hg(II), Pb(II), Co(II), Ni(II), Mn(II), Mn(IV), Fe(II), Cu(I), Cu(II), Fe(III), Al(III) and Cr(III).

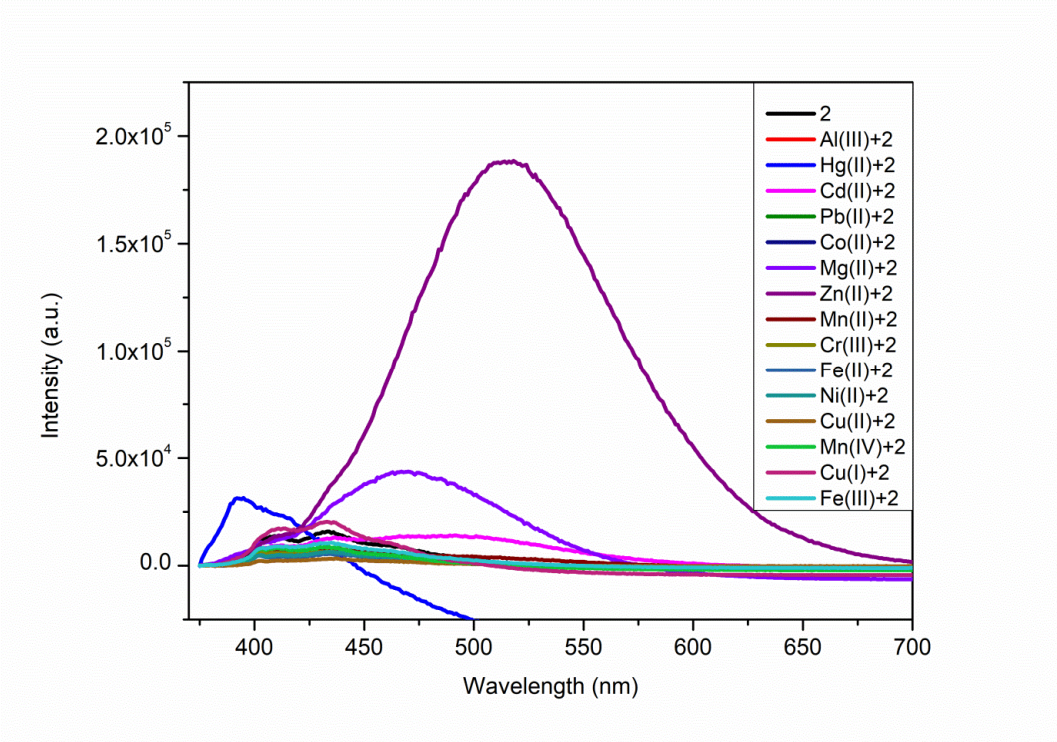

Fig. 4. Fluorescence spectra of **2** with metal ions Mg(II), Zn(II), Cd(II), Hg(II), Pb(II), Co(II), Ni(II), Mn(II), Mn(IV), Fe(II), Cu(I), Cu(II), Fe(III), Al(III) and Cr(III).

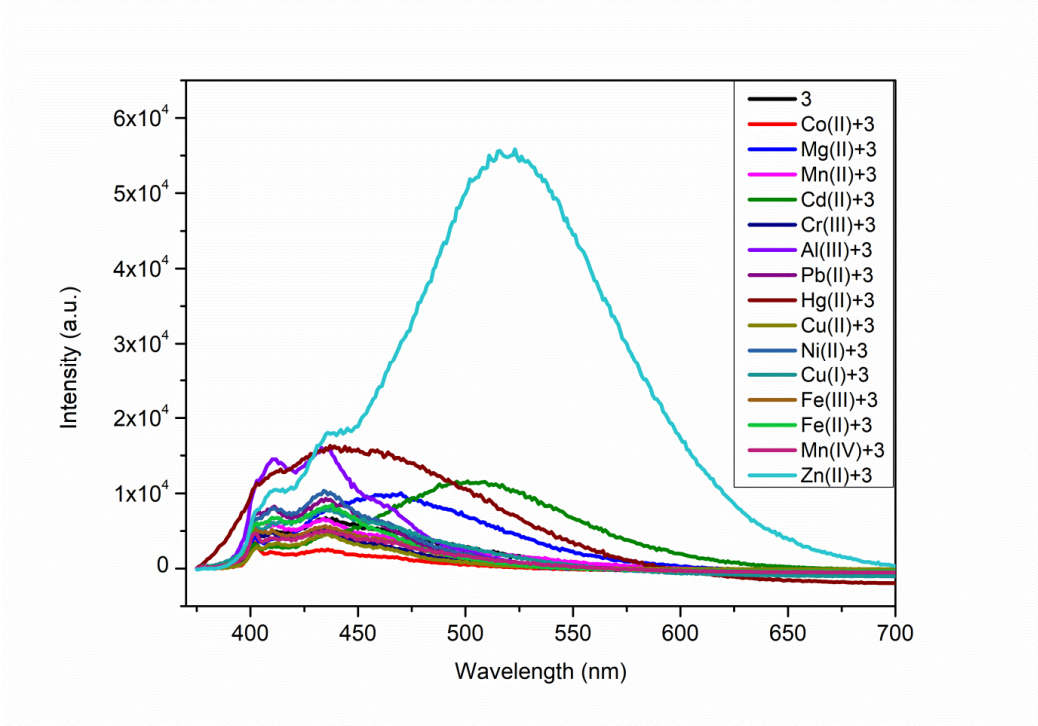

Fig. 5. Fluorescence spectra of **3** with metal ions Mg(II), Zn(II), Cd(II), Hg(II), Pb(II), Co(II), Ni(II), Mn(II), Mn(IV), Fe(II), Cu(I), Cu(II), Fe(III), Al(III) and Cr(III).

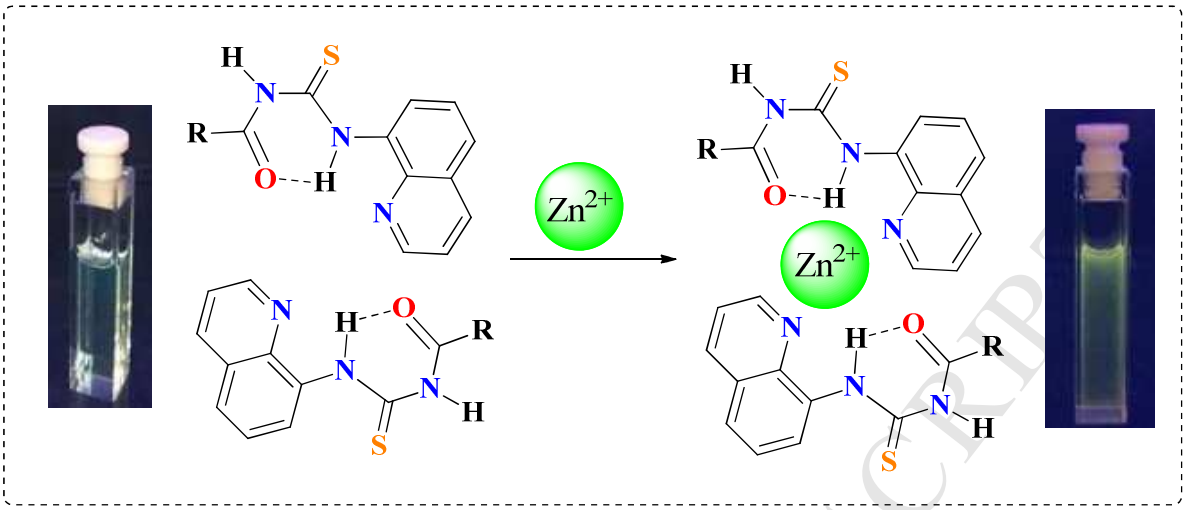

Scheme 2. Illustration of the interaction of acylthiourea with Zn^{2+}.

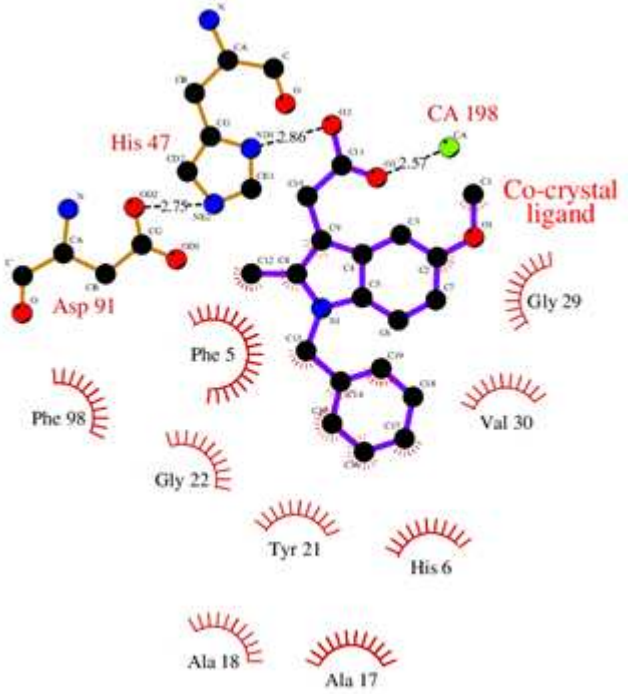

Co-crystal

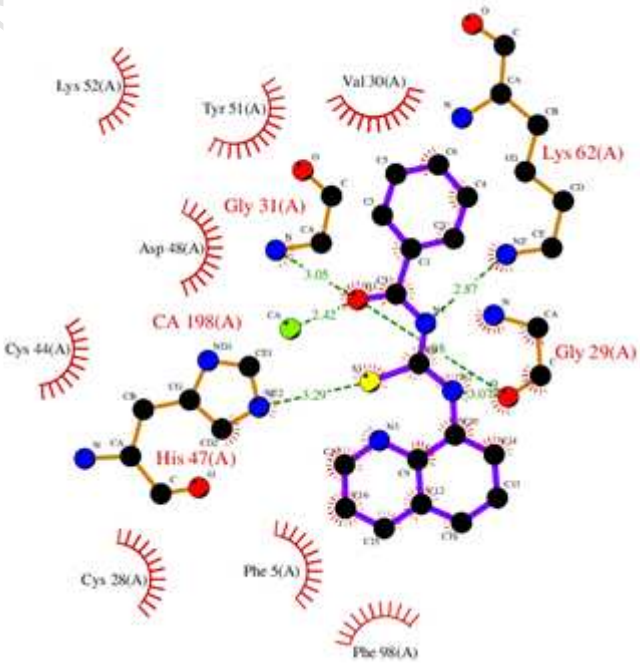

Compound **1**

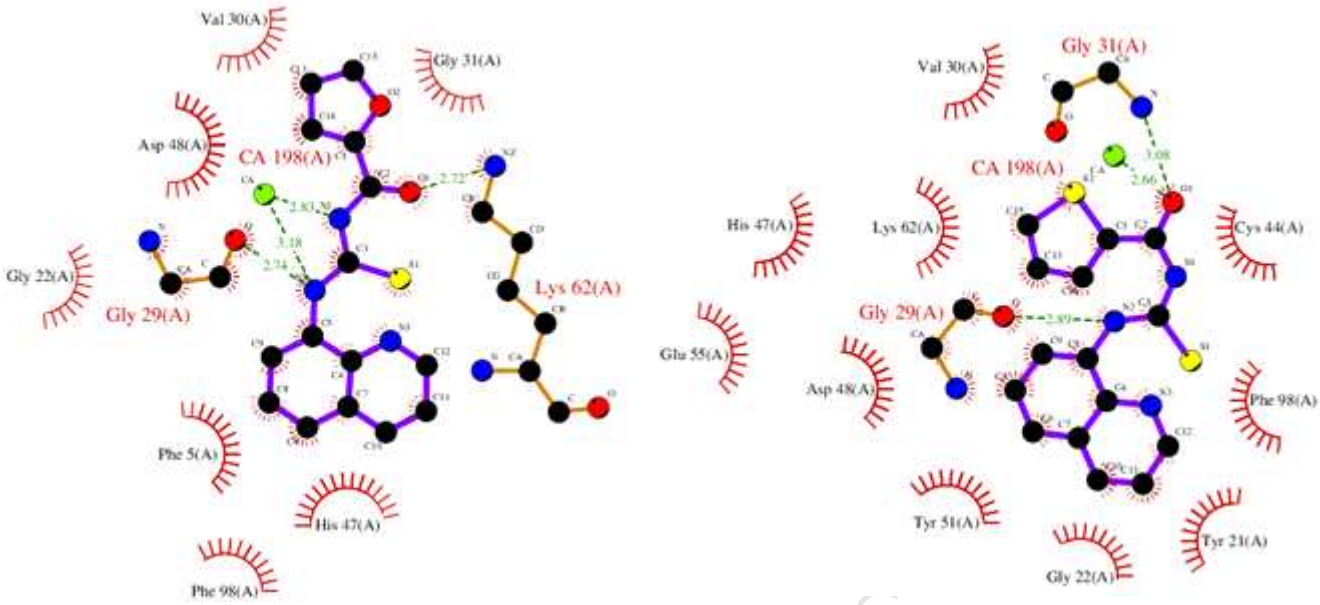

Fig. 6. Ligplot representation showing hydrogen bonding and hydrophobic interactions at the active site of non-pancreatic secretory PLA2 by co-crystal ligand ((1-benzyl-5-methoxy-2-methyl-1h-indol-3-yl)acetic acid) and compounds **1**-**3**.

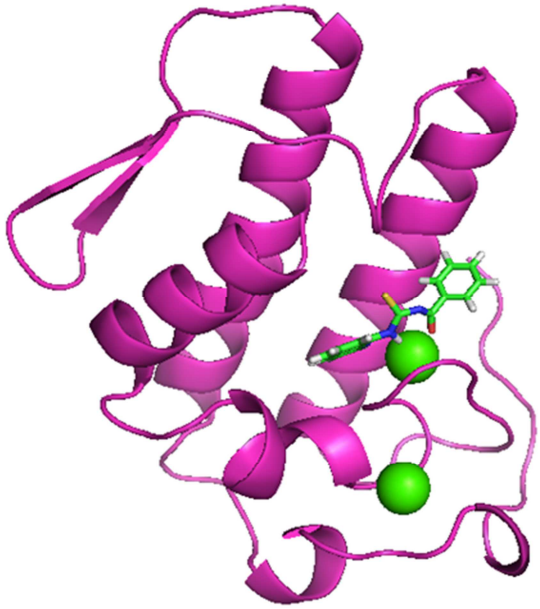

Fig. 7. Compound **1** bound at the active site of non-pancreatic secretory PLA2.

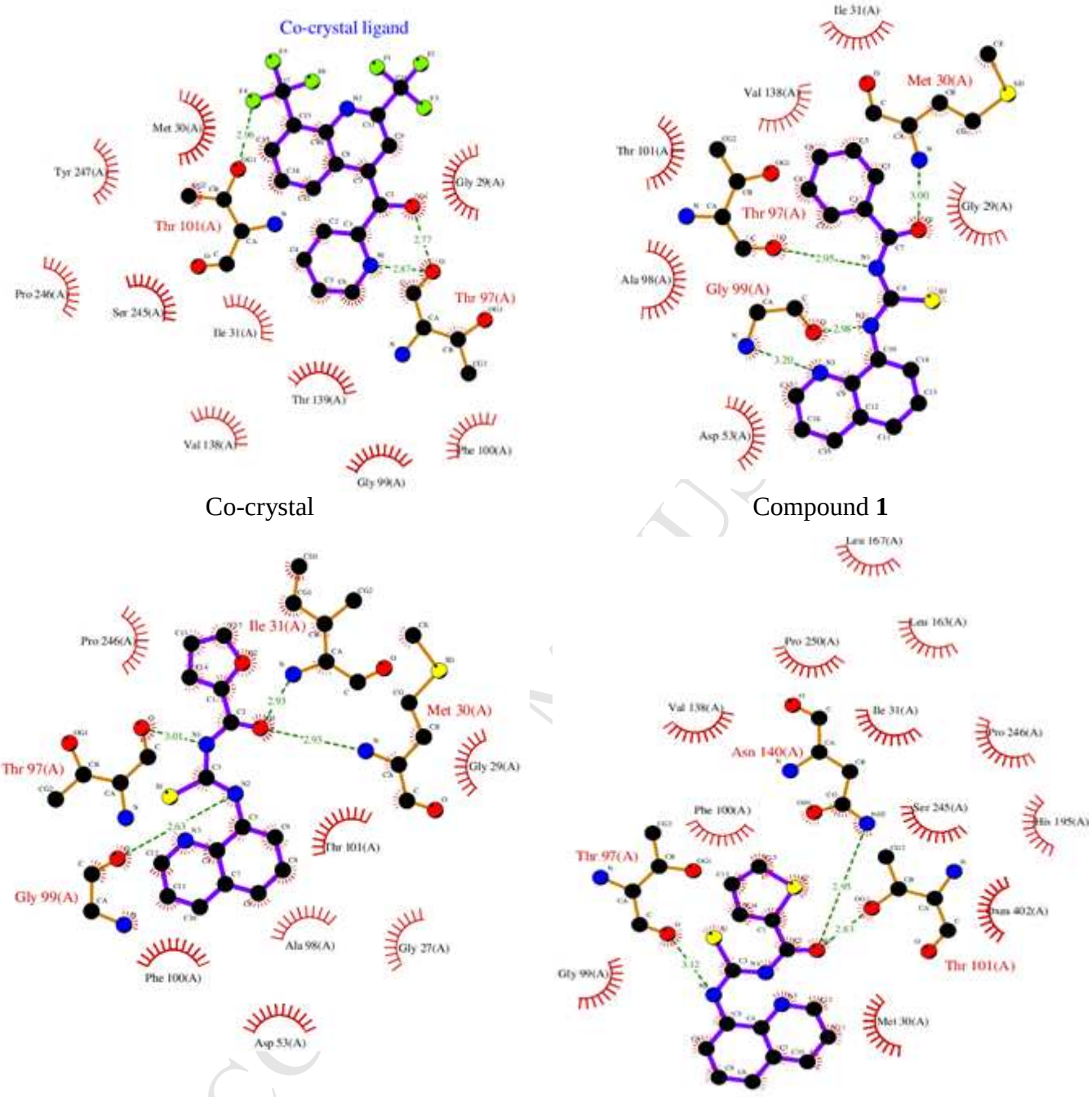

Fig. 8. Ligplot representation showing hydrogen bonding and hydrophobic interactions at the active site of lactate dehydrogenase by co-crystal ligand (1,4-dihydronicotinamide adenine dinucleotide) and compounds **1**-**3**.

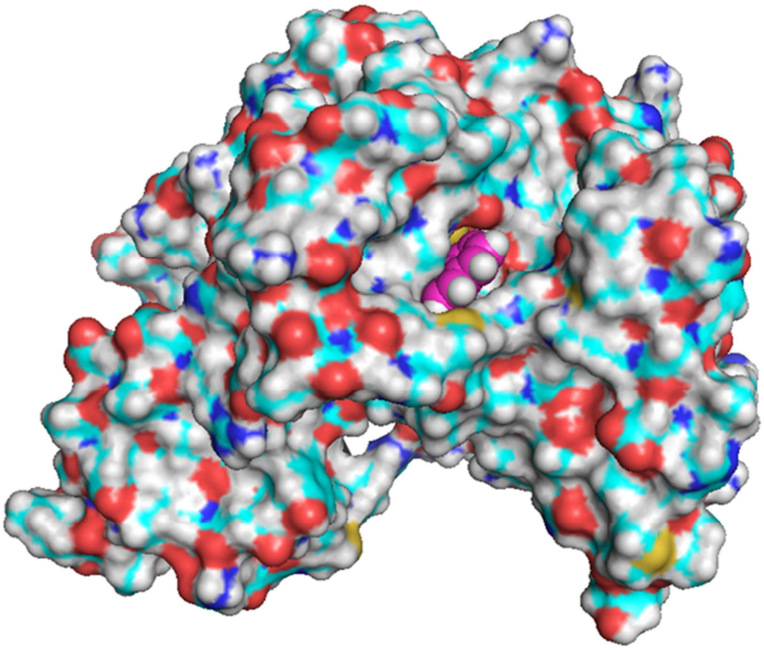

Fig. 9. Surface view of lactate dehydrogenase with compound **3** bound at the active site.

ACCEPTED MANUSCRIPT

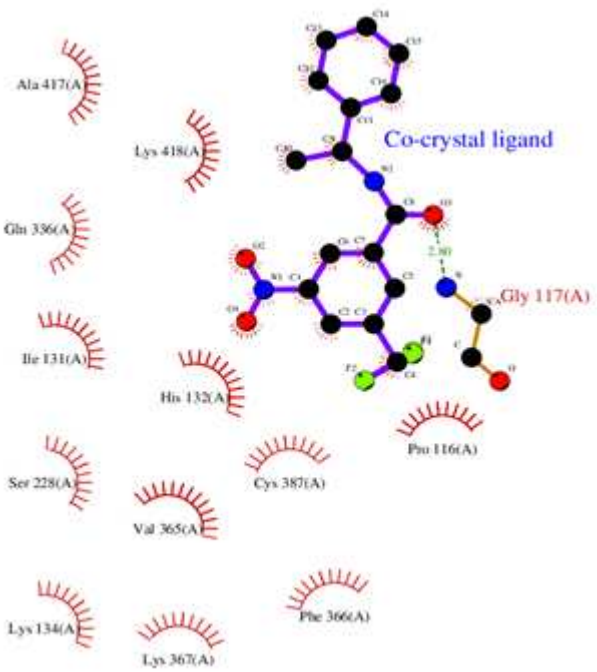

Co-crystal

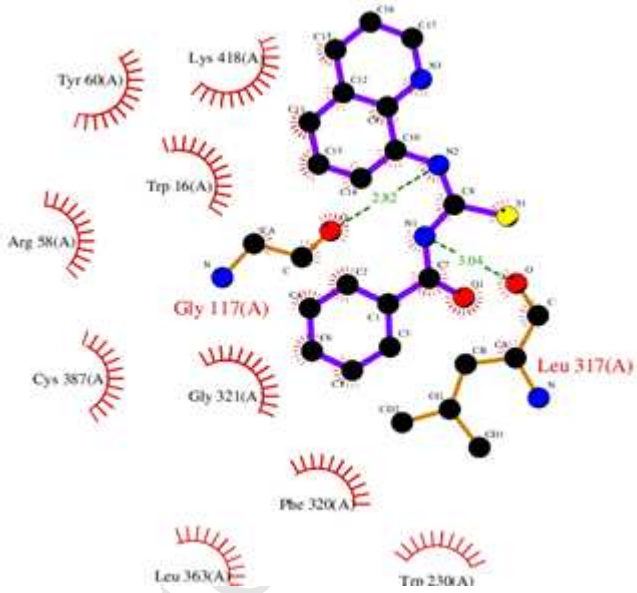

Compound **1**

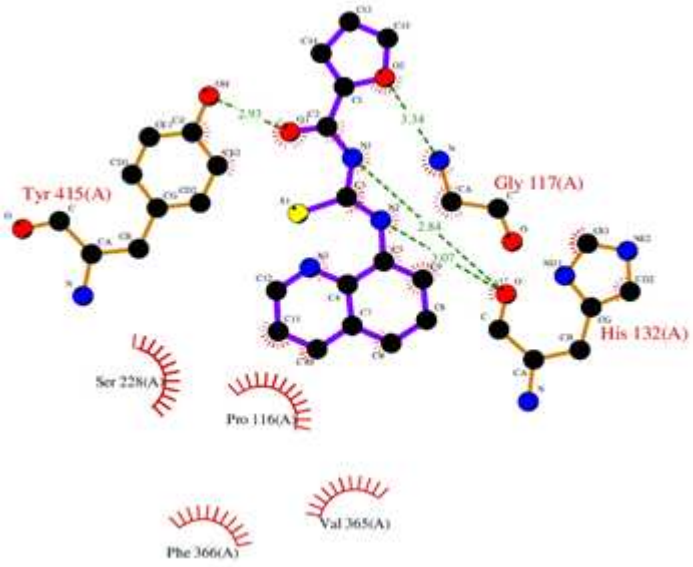

Compound **2**

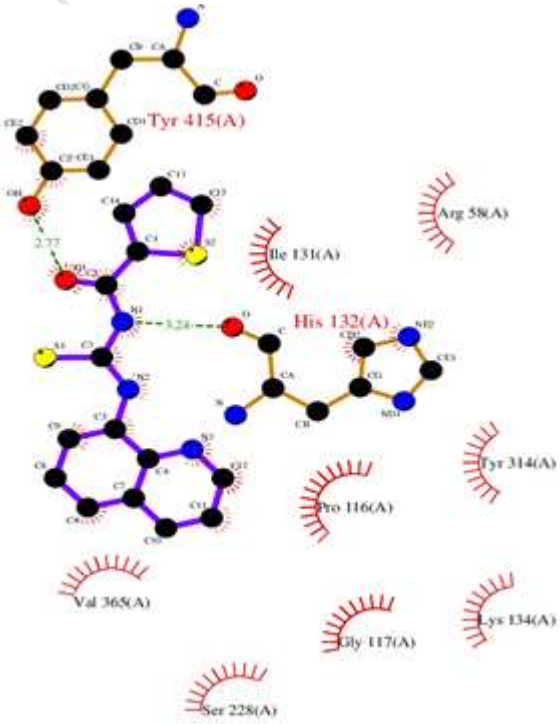

Compound **3**

Fig. 10. Ligplot representation showing hydrogen bonding and hydrophobic interactions at the active site of DprE1 by co-crystal ligand (3-nitro-N-[(1R)-1-phenylethyl]-5-(trifluoromethyl)benzamide) and compounds **1-3**.

ial Use Only

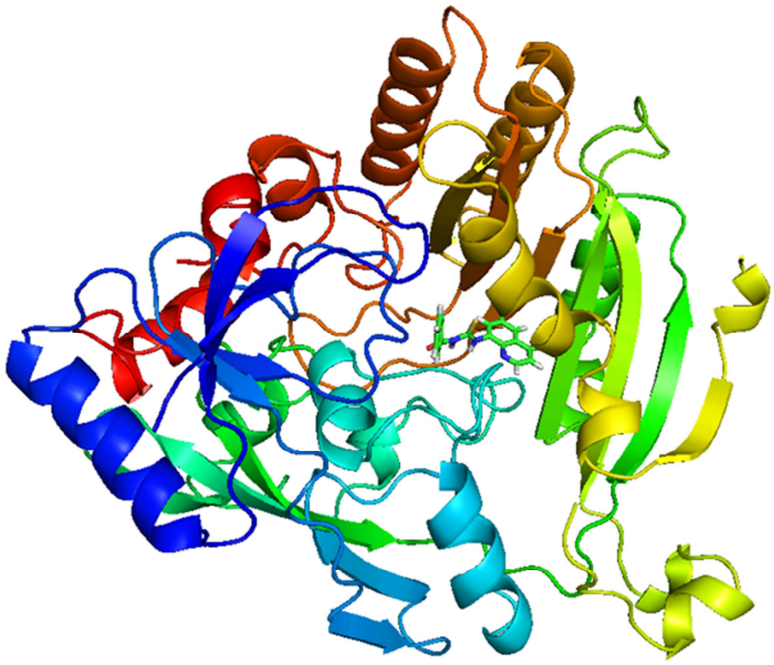

Fig. 11. Representation of DprE1 with compound **1** bound at the active site.

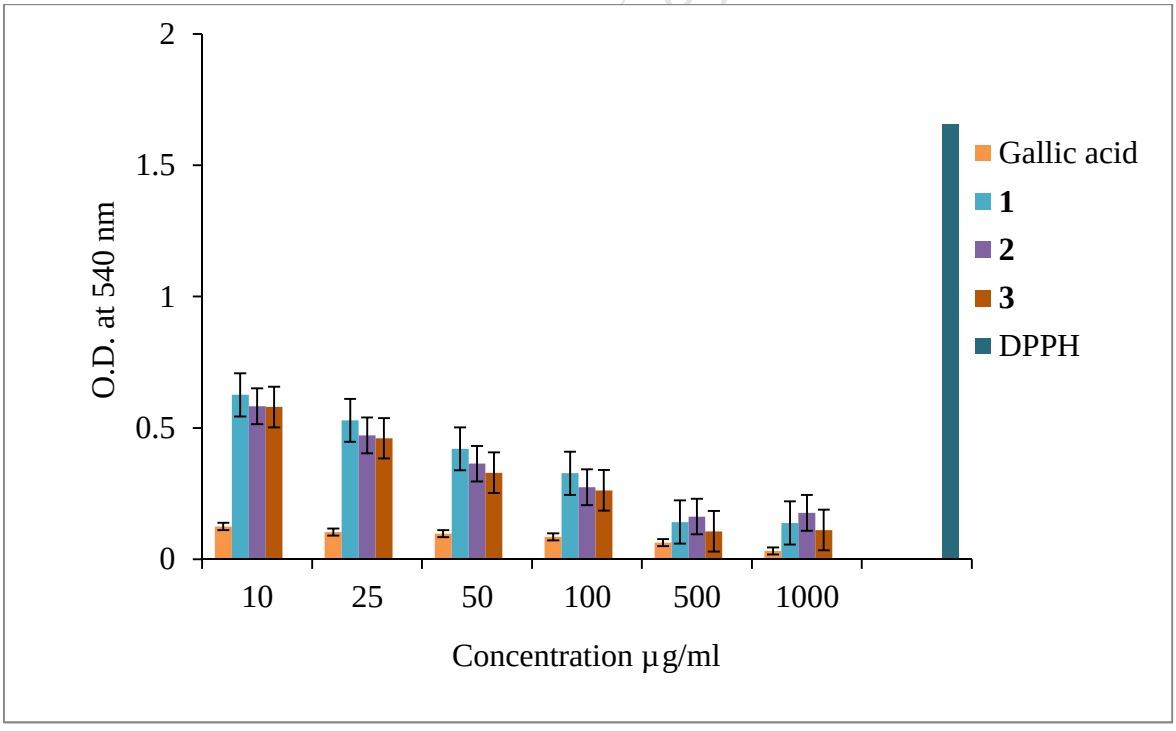

Fig. 12. DPPH assay of the compounds (**1-3**).

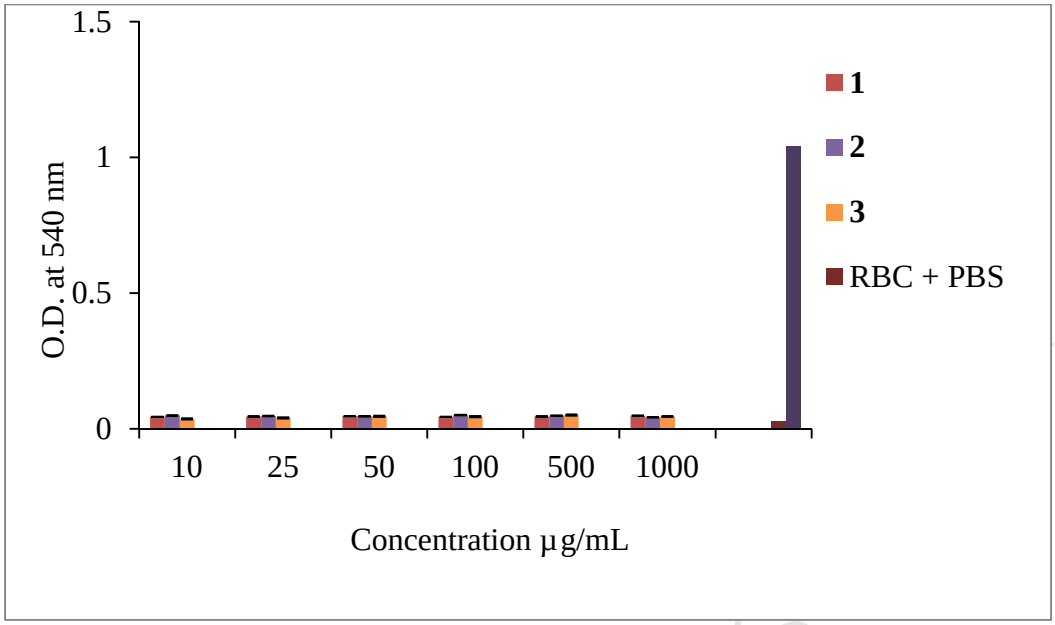

Fig. 13. Haemolysis assay of the compounds (**1-3**).

ACCEPTED MANUSCRIPT

ACCEPTED MANUSCRIPT

Table 1. Crystallographic data and refinement parameters

	1	**3**
Chemical formula	$C_{17}H_{13}N_3OS$	$C_{15}H_{11}N_3OS_2$
M_r	307.36	313.39
Crystal system, space group	Monoclinic, $P2_1/n$	Monoclinic, $P2_1/n$
Temperature (K)	100.0	100.0
Unit cell dimensions	a = 10.2772(2) Å	a = 9.9317(5) Å
	b = 4.80670(10) Å	b = 4.8302(2) Å
	c = 28.6407(7) Å	c = 28.4859(14) Å
	α = 90°	α = 90°
	β = 92.1460(10)°	β = 91.320(2)°
	γ = 90°	γ = 90°
V (Å^3)	1413.84(5)	1366.17(11)
Z	4	4
Absorption coefficient μ (mm^{-1})	1.444	3.548
F(000)	640	648
Crystal size (mm)	0.434 × 0.201 × 0.058	0.424 × 0.36 × 0.138
Radiation type	Cu *Kα* radiation	
Wavelength (Å)	1.54178	1.54178
Diffractometer	BRUKER VENTURE (KAPPA)9	
Measured reflections	24273	14854
Independent reflections	2673	2571
Reflections with I > 2σ(I)		
R_{int}	0.0366	0.0364
θ_{max}, θ_{min} (°)	70.207, 3.088	70.145, 3.103
h	–12<=h<=11,	–12<=h<=12,
k	–5<=k<=4,	–4<=k<=5,
l	–34<=l<=34	–33<=l<=34
Absorption correction	Semi-empirical from equivalents	
Refinement method	Full-matrix least-squares on F^2	
No. of reflections /	2673 / 0 / 199	2571 / 0 / 190

parameters

R indices [$F^2 > 2\sigma(F^2)$]	R1 = 0.0320, wR2 = 0.0790	R1 = 0.0361, wR2 = 0.0892
R indices (all data)	R1 = 0.0366, wR2 = 0.0817	R1 = 0.0380, wR2 = 0.0905
Goodness of fit on F^2 (S)	1.084	1.074
$\Delta\rho_{max}$, $\Delta\rho_{min}$ (e Å^{-3})	0.229 and –0.271	0.271 and –0.468

Table 2. Bond lengths (Å) and angles (°) for **1** and **3**

	1	**3**
S(1)–C(10)	1.6754(14)	1.6805(18)
O(1)–C(11)	1.2230(18)	1.223(2)
N(1)–C(1)	1.3200(19)	1.317(2)
N(1)–C(5)	1.3663(18)	1.368(2)
N(2)–H(2)	0.8800	0.8800
N(2)–C(9)	1.4095(18)	1.409(2)
N(2)–C(10)	1.3366(19)	1.337(2)
N(3)–H(3)	0.8800	0.8800
N(3)–C(10)	1.3982(18)	1.394(2)
N(3)–C(11)	1.3812(18)	1.382(2)
S(2)–C(12)	-	1.7256(18)
S(2)–C(15)	-	1.708(2)

Table 3. Torsion angles (°) for **1** and **3**

	1	**3**
N(1)-C(5)-C(9)-N(2)	0.75(19)	3.0(2)
C(9)-N(2)-C(10)-S(1)	-0.1(2)	1.0(3)
C(9)-N(2)-C(10)-N(3)	-179.18(13)	-178.49(16)
C(10)-N(3)-C(11)-O(1)	-3.6(2)	-2.4(3)
C(11)-N(3)-C(10)-S(1)	-179.36(12)	-178.99(14)
C(11)-N(3)-C(10)-N(2)	-0.2(2)	0.5(3)
N(3)-C(11)-C(12)-S(2)	-	-164.86(12)

ACCEPTED MANUSCRIPT

Table 4. Inter- and intra-molecular hydrogen bonds (Å and °) in **1** and **3**

D-H...A	d(D-H)	d(H...A)	d(D...A)	<(DHA)
Compound **1**				
N(2)-H(2)...O(1)	0.88	1.89	2.6304(15)	140.4
N(2)-H(2)...N(1)	0.88	2.18	2.6356(17)	112.0
N(3)-H(3)...S(1)#1	0.88	2.84	3.6340(12)	151.2
Compound **3**				
N(2)-H(2)...O(1)	0.88	1.91	2.650(2)	140.2
N(2)-H(2)...N(1)	0.88	2.18	2.641(2)	111.9
N(3)-H(3)...S(1)#1	0.88	2.72	3.4597(14)	142.0

Symmetry transformations used to generate equivalent atoms:

#1 -x+1,-y+1,-z+1

ACCEPTED MANUSCRIPT

Table 5. Docking energy, glide score, hydrogen bonds and hydrophobic interactions at the active site of the enzymes

Compounds	Energy (kcal/mol)	Docking score	Hydrogen bonding interaction	Hydrophobic interactions
1-benzyl-5-methoxy-2-methyl-1H-indol-3-yl-acetic acid	–50.552	–7.551	Ca^{2+}, His47	Phe5, His6, Ala17, Ala18, Tyr21, Gly22, Gly29, Val30, Phe98
1	–53.590	–7.398	Ca^{2+}, Gly29, Gly31, His47, Lys62	Phe5, Cys28, Val30, Cys44, Asp48, Tyr51, Lys52, Phe98
2	–49.329	–8.076	Ca^{2+}, Gly29, Lys62	Phe5, Gly22, Val30, Gly31, His47, Asp48, Phe98
3	–52.191	–9.093	Ca^{2+}, Gly29, Gly31	Tyr21, Gly22, Val30, Cys44, His47, Asp48, Tyr51, Glu55, Lys62, Phe98
Mefloquine	–45.562	–6.063	Thr97, Thr101	Gly29, Met30, Ile31, Gly99, Phe100, Val138, Thr139, Ser245, Pro246, Tyr247
1	–51.620	–6.230	Met30, Thr97, Gly99	Gly29, Ile31, Asp53, Ala98, Thr101, Val138
2	–51.612	–5.733	Met30, Ile31, Thr97, Gly99	Gly27, Gly29, Asp53, Ala98, Phe100, Thr101, Pro246
3	–58.492	–7.016	Thr97, Thr101, Asn140	Met30, Ile31, Gly99, Phe100, Val138, Leu163, Leu167, His195, Ser245, Pro246, Pro250
3-nitro-N[(1R)-1-phenylethyl]-5-(trifluoromethyl) benzamide	–41.76	–6.77	Gly117	Pro116, Ile131, His132, Lys134, Ser228, Gln336, Val365, Phe 366, Lys367, Cys387, Ala417, Lys418
1	–57.295	–9.135	Gly117, Leu317	Trp16, Arg58, Tyr60, Trp230, Phe320, Gly321, Leu363, Cys387, Lys418
2	–53.931	–9.148	Gly117, His132, Tyr415	Ser228, Pro116, Val365, Phe366
3	–56.500	–7.733	Tyr415, His132	Arg58, Pro116, Gly117, Ile131, Lys134, Ser228, Tyr314, Val365

ACCEPTED MANUSCRIPT

ACCEPTED MANUSCRIPT

Highlights

- Synthesis and characterization of 8-aminoquinoline based aroylthiourea compounds
- Metal ion sensing ability of the compounds was studied by various spectroscopic tools
- Aroylthiourea derivatives showed good antioxidant activity
- Antimalarial, antiinflammatory and antituberculosis potentials were verified by molecular docking

ACCEPTED MANUSCRIPT